

Intelligent Object Grasping With Sensor Fusion for Rehabilitation and Assistive Applications

Brielle J. B. Lee, Adam Williams, and Pinhas Ben-Tzvi^{ID}, *Senior Member, IEEE*

Abstract—This paper presents the design and control of the intelligent sensing and force-feedback exoskeleton robotic glove to create a system capable of intelligent object grasping initiated by detection of the user's intentions through motion amplification. Using a combination of sensory feedback streams from the glove, the system has the ability to identify and prevent object slippage, as well as adapting grip geometry to the object properties. The slip detection algorithm provides updated inputs to the force controller to prevent an object from being dropped, while only requiring minimal input from a user who may have varying degrees of functionality in their injured hand. This paper proposes the use of a high dynamic range, low cost conductive elastomer sensor coupled with a negative force derivative trigger that can be leveraged in order to create a controller that can intelligently respond to slip conditions through state machine architecture, and improve the grasping robustness of the exoskeleton. The improvements to the previous design are described while the details of the controller design and the proposed assistive and rehabilitative applications are explained. Experimental results confirming the validity of the proposed system are presented. Finally, this paper concludes with topics for future exploration.

Index Terms—Exoskeletons, grasping, slip detection, rehabilitation robotics, upper limb.

I. INTRODUCTION

NUMEROUS illnesses and injuries may lead to impaired hand functionality, from stroke to cerebral palsy to impact injuries that result to fractures and nerve damage. Loss of hand dexterity and strength often causes a drastic decrease in the patient's quality of life, and makes it difficult to perform activities of daily living (ADL). Illnesses and injuries in combination with an aging population will drive future increases in rate of the patients who need rehabilitation and assistance, resulting in greater demand for healthcare services and a rise in related costs [1].

Common treatment aimed at returning hand functionality following such an illness or injury often includes some form of rehabilitation treatment. This involves performing strength training exercises and dexterity building activities, usually overseen by a licensed occupational therapist. While the frequency and intensity of active rehabilitation increases the rate of recovery, involvement in this level of rehabilitation can

Manuscript received January 7, 2018; revised April 5, 2018 and May 16, 2018; accepted June 3, 2018. Date of publication June 18, 2018; date of current version August 7, 2018. (Corresponding author: Pinhas Ben-Tzvi.)

The authors are with the Robotics and Mechatronics Laboratory, Virginia Tech, Blacksburg, VA 24061 USA (e-mail: bentzvi@vt.edu).
Digital Object Identifier 10.1109/TNSRE.2018.2848549

often be limited due to the cost or difficulty in attending such sessions for injured or elderly patients [1], [2]. Similarly, passive rehabilitation, through guided motions, can alleviate joint pain while helping the patients to combat muscle and bone atrophy prior to beginning active rehabilitation, or maintain progress once active rehab has begun [2]. However, as passive rehabilitation requires another person or device to perform the exercises on the patients, the access is again limited. This challenge has led to the expansion of research into using assistive robotic technology to improve the accessibility of rehabilitative services for hard to reach demographics [3]–[6].

In addition to the exploration of rehabilitative devices, a complementary active research topic is the investigation of utilizing assistive wearable gloves and orthoses that serve to augment and amplify the abilities of the wearer. Whether improving grip strength and reducing fatigue like the NASA/GM RoboGlove [7] or aiding persons with impaired hand mobility to grasp everyday objects with soft robotic gloves, these systems are intended to be worn by the targeted user to improve their manual capabilities [8]. While the earliest robotic exoskeleton gloves had large footprints and were heavy to use, the focus has been in the reduction in weight, size, and actuation requirements in order to increase the adoption of the use of robotic assistive devices. However, there are tradeoffs made in the design of such systems. For instance, while soft systems are often lightweight, they also incorporate the use of fluidic actuation systems that then require the inclusion of a pump or compressor. Hard frame exoskeletons on the other hand struggle to maintain a feasible weight and face actuation hurdles as well with large battery packs/actuation units.

Key in the design of these platforms is the intended motions and interactions of the user. These then inform not only the physical design process, but the design of the control and operation of the system as well. In many cases, a force control paradigm is used, whether implemented via PID, impedance control, sliding mode control, or some other paradigm [9]–[11]. However, this method depends on the prior calibration or calculation of what the required force input must be for successful motion, grasping, interaction, or other desired action. In addition, the wearer must have the sensory and control capability to adjust the force input if the action is unsuccessful. Even when possible, this may prove difficult at times for wearers with broader impairment. For these reasons, robotic exoskeletons would greatly benefit from further exploration of intelligent grasping paradigms.

Outside of the realm of robotic exoskeletons, there has been far more extensive research into intelligent grasping as

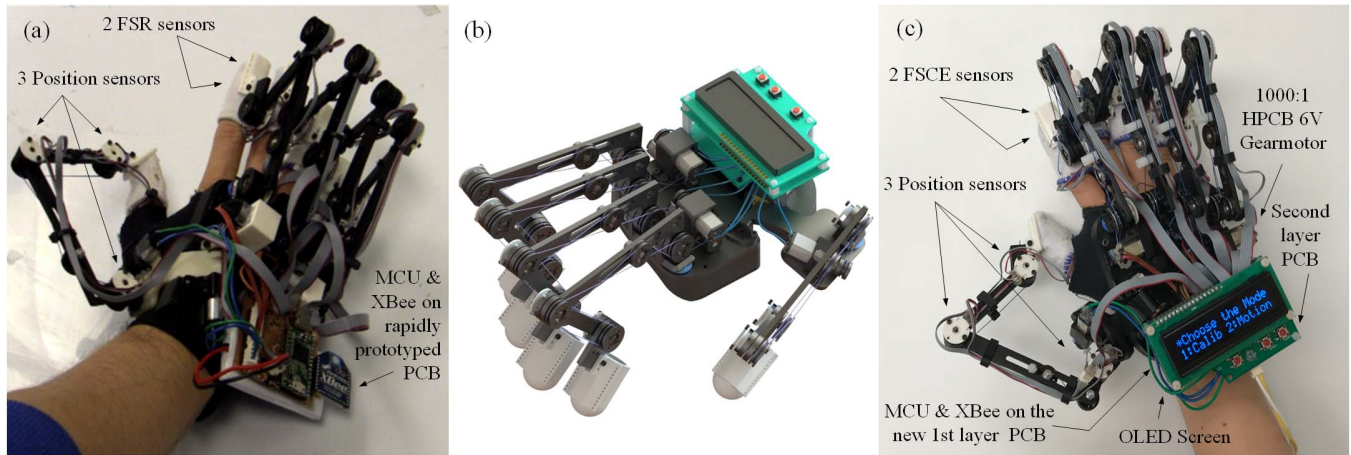


Fig. 1. (a) Original components of the SAFER glove [21] (b) New 3D CAD model with updated components (c) Updated components of the iSAFER glove.

applied to robotic manipulators and prosthetics. One of the key elements of intelligent grasping is the detection of slip conditions, as this signals a failure in the grasp that is then utilized to trigger an error correction behavior [12]–[16]. The extant work in robotic hand provides a basis for the application of a slip-aware intelligent grasping paradigm to a robotic exoskeleton for the first time.

This paper proposes the use of a high dynamic range, low cost conductive elastomer sensor coupled with a negative force derivative trigger that can be leveraged in order to create a controller that can intelligently respond to slip conditions through a state machine architecture, and improve the grasping robustness of the exoskeleton. In order to perform experimental validation, modifications and updates have been made to the SAFER glove. The improvements to the robotic glove exoskeleton are described in section II, while section III details the controller design as well as the proposed assistive and rehabilitative applications. Section IV presents the results of the performed experiments, and section V provides a conclusion as well as proposes topics for future exploration.

II. GLOVE MECHANISM SYSTEM DESIGN

The sensing and force-feedback robotic (SAFER) glove was designed and experimentally validated in previous work as an assistive and rehabilitative aid [9], [17]–[25]. The SAFER glove shown in Fig. 1(a) consists of articulated linkages that each drive a finger through a cable routing system that ultimately are actuated by miniature DC motors. Antagonistic routing provides full controllability of the system. The next sections will further describe the mechanical design and system of the SAFER glove and the motivation and design evolution of the original system.

A. Mechanical Design and system of SAFER

The multi-link finger mechanism produces flexion and extension at the proximal joints, and the glove mechanism configuration can be adjusted in order to accommodate different finger lengths. Through optimization, the optimal link length

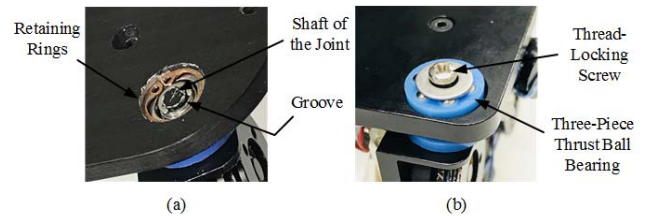


Fig. 2. (a) Joint of SAFER glove (b) New robust joint of iSAFER glove.

for a multi-link finger mechanism with bidirectional tendon actuation was modeled considering workspace size, force transmission ratio, and mechanical design parameters [19]. Each finger has two force-sensitive resistors (FSR) on both the pad and the fingernail of the fingertip thimble of SAFER to measure force applied to fingers and three potentiometers on each joint to calculate the fingertip position [25]. The actuators, controller, and power supply are mounted upon a lightweight platform that is worn on the back of the hand. The self-contained nature of the system lends a high degree of portability to the system. Furthermore, it also has the wireless communication capability with a PC for increased portability.

B. Design Changes to the System

In order to improve the stability, strength, and sensing capabilities of the system, improvements and modifications were made in the following areas to the previously described SAFER design, resulting in an intelligent SAFER (iSAFER) glove pictured in Fig. 1(b) above.

1) *More Stable and Robust Joints*: To achieve the lightest weight possible, most of the exoskeleton components are manufactured from 6061 aluminum. However, due to the aluminum's softness and the small profile of the linkages, the retaining ring grooves quickly wore out at the major joints. To fix these weak spots, a new joint was designed that would maintain the original functionality. Instead of the retaining ring with the groove on the outside of the shaft, a hole was drilled in the shaft, and then the thread-locking screws were used with additional three-piece thrust ball bearings to keep the free rotation feature as shown in Fig. 2. Increased thickness

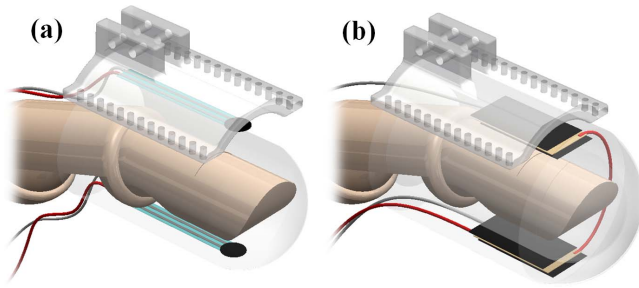


Fig. 3. (a) FSR sensors in and outside of the single layer thimble for SAFER (b) FSCE sensors in between two layers of thimbles for iSAFER.

was still well maintained within the base plates of the iSAFER glove on dorsum of the hand.

2) *New Force-Sensitive Conductive Elastomer Sensors:* Preliminary testing on the previously used FSR sensor showed that it was not suitable for all the desired functional modes. This FSR sensor had a 4 mm diameter active sensing area utilized to detect the force created between the finger and an object. Depending on the point where the force was applied on the finger, the FSR sensor would at times fail to detect the force if the application of force did not align properly with the sensor position.

At first, replacing the FSR with a larger size of the same model was considered, however the stiff plastic cover on the sensor limited the applicability to a fingertip. Even with the original, smaller sensor, shown in Fig. 3(a), a repetitive bending motion of the finger caused a tear in the sensor requiring a replacement, and as the sensor gets bigger, the risk of damage and the stiffness of the sensor on the fingertip rendered this option impractical.

As a result, a custom-made sensor that could accommodate the shape and the size of a fingertip and was durable across multiple bending motions was required. To meet these goals, a sheet made out of a polymeric foil impregnated with carbon black, called Velostat, was layered with fine metallic mesh on both sides in order to create the force-sensitive conductive elastomer (FSCE) sensor. Velostat possesses a linearly varying conductivity relative to pressure, which makes it ideal for a new custom-made FSR sensor, FSCE sensor. By utilizing the voltage divider circuit with a resistor, resistance of the sensors were converted into a voltage, then force. The benefits of the FSCE sensor are the larger sensing surface, cheaper cost to produce, more resilient, and higher sensitivity than the previous FSR. The FSCE sensors were then inset on both the pad and the fingernail of the fingertip thimble of the iSAFER glove as shown in Fig. 3(b). In order to calibrate the sensor, masses were applied to a test sensor affixed to a scale. The resultant scale factor was found to be 1.74 N/V.

3) *Upgraded Electronic Interfaces:* The original rapidly prototyped printed circuit board (PCB) on Fig. 1(a) was replaced with custom manufactured PCB. In order to improve the interface between the user and the glove, a new second layer PCB was designed to accommodate the addition of an OLED screen, three buttons, and an inertial measurement unit (IMU). To fit the system on top of the dorsum of the hand and keep

the original form factor, the additional PCB was designed to be located on top of the base PCB. These two boards share the power source, and communicate through one Teensy on the base PCB.

Two of the buttons are used to initiate the changes between the state machines, while the third is implemented as an emergency stop that returns the glove to the idle state when pressed. The IMU is added to detect the hand rotation and position in relation to the wrist and arm position in future work.

In addition, the original motors were replaced with 6V 1:1000 high power miniature gearmotors with long-life carbon brushes (HPCB). The XBee wireless unit was securely relocated to the bottom of the original PCB to reduce the physical damage to the electronic system. When grasping a short object on a table, the little finger side of the hand often touches the table. The location of the Xbee in the previous design, as seen in Fig. 1(a), caused external impact on the Xbee while it acted as an obstruction.

III. REHABILITATION AND ASSISTIVE SYSTEM OF THE GLOVE

Recovery from debilitating hand injury is generally evaluated through Modified Ashworth Scale (MAS) rated on a 0-5 scale [26], [27]. Previous work with this platform proposed techniques for passive rehabilitation, through repeated passive motion guidance from a learned library of hand motions corresponding to grasps learned from a collection of healthy hand motions, coupled with active resistive rehabilitation through leveraging the glove's haptic feedback capabilities [25]. The current work expands previous functionalities, through the inclusion of grasping assistance as well as user-initiated passive grasping motions. This type of robot-assisted rehabilitation has been shown to result in favorable outcomes such as noticeable reduction in spasticity, decreasing the MAS score of joints, and small increases in the Rivermead Motor Assessment for subacute stroke survivors [27]. In a similar way, the study with MIT-Manus interacted with stroke patients actively and/or passively and showed statistically significant improvement including favorable trends in strength change, Fugl-Meyer Scale, and motor status scale [28]. Thus, robotic rehabilitative aids can greatly benefit a patient recovering from loss of dexterity or strength in their hand.

The iSAFER system is designed to have different modes that can perform either passive or active rehabilitation. In general, passive exercise can benefit patients in all MAS levels to alleviate atrophy, while also a necessary rehabilitation exercise for the patients at MAS level 0. Once the patients advance to level 1 and have the capability to initiate minor muscle activation, such as a twitch, active rehabilitation with adjustable resistance can be applied depending on the level of the recovery from the injuries.

A. Intelligent Object Grasping Rehabilitation System Overview

Simple force control of an exoskeleton requires an informed input force for the system. However, in real life, people not

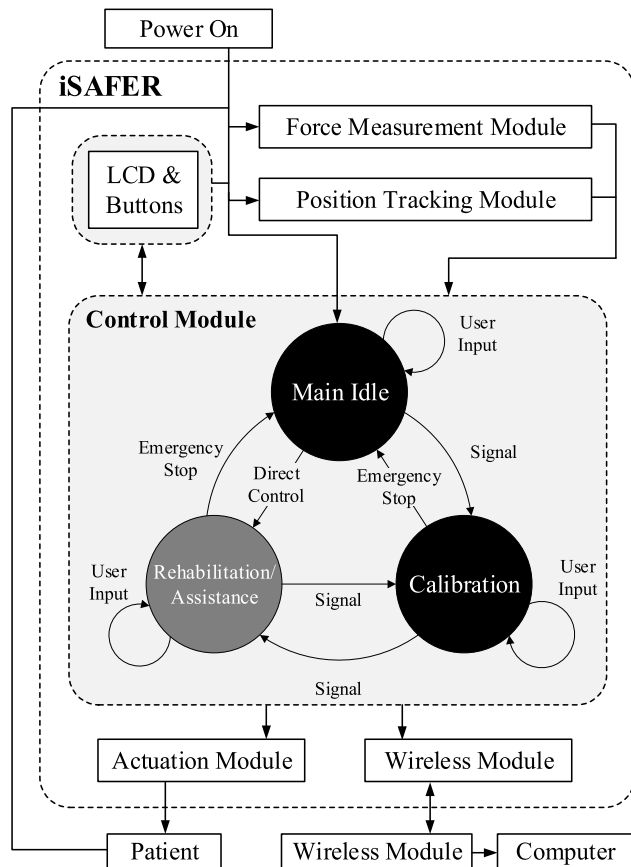


Fig. 4. Operational flowchart for the iSAFER glove.

only interact with rigid objects, i.e. a glass cup, but also with deformable objects, i.e. a paper cup. In this analogy, an overly firm grasp of a paper cup can easily result in crushing and spillage of the cup. With this in consideration, the iSAFER glove has been developed to provide a wide range of acceptable grip forces by applying a soft initial force and then adapting to the environment and the object through the detection of slip conditions. A discrete, minute force step increase is applied when slip is detected, and continuously applied until the system detects that it is no longer in a slip condition. In order to maintain programmatical simplicity and provide an expandable operational paradigm, the system is designed to be finite state machine. The system overview is shown in Fig. 4. The system consists of the three state machines: Calibration, Active Rehabilitation and Assistance, and Main Idle. The method of activation for the system was given considerable thought during the design of the controller. For patients possessing some degree of bilateral paralysis or weakness, using a switch or EMG, for example, could require extensive rehabilitation just to regain this function. The current system instead uses motion amplification as its primary activation mode, referred to here as a “twitch” signal. The glove’s FSCE sensors are capable of detecting even minor force fluctuations and treat inward or outward forces, relative to the finger pad, as a signal to close or open the fist, respectively. The control can then be adjusted to filter oscillatory signals, as well as to increase or decrease the

activation force threshold, to accommodate patients who may have tremors or imprecise motion early in their rehabilitation.

While a small initial grasp force is of value when interacting with deformable objects, humans generally respond to tactile vibrational signals to gauge required force and adjust dynamically as required to interact with an object [29]. To continue the previous analogy, an empty paper cup can be grabbed without a slippage with a very small force, but should it be filled with water, this small force will no longer be sufficient. Therefore, detecting the shape, surface roughness or orientation alone may result in failed grasps unless the exoskeleton applies its maximum feasible force on the object in all cases in order to preclude any slippage. Therefore, the functional design of the iSAFER glove is more similar to the biological evaluation of grip stability.

A basic outline of the operational structure of the iSAFER glove is as follows: The system initially applies a calculated minimum force. Should the object shift within the grip of the glove, it will detect the slippage. Once the slippage detection is triggered, the grip force will be adjusted until the object no longer slips.

B. State Machine Architecture

The initial and main operative state for the glove following powering on is the Main Idle. While in Main Idle, the fingers will remain at rest in the current position, and the system will wait for a command. When the emergency stop button is pressed in any other states or cases, the system will come back to this Main Idle state while resetting all the saved sensor, state, or case data.

The second state is the Calibration state. A hurdle faced in previous iterations of the glove is adapting the system to variously sized hands. The glove has the ability to be fit to a variety of hand widths and thicknesses through its design; however, the control will vary with the hand geometry. Therefore, in order to take into account the initial pressure applied to the FSCE sensors due to variations in wearer, the glove must initially move to a calibration state machine.

In Calibration, the iSAFER glove performs warm up rehabilitation motions while simultaneously learning the minimum force values of each fingers. These motions progress through multiple concerted and individual flexions and extensions, in order to both provide a full stretch for the patient’s fingers and hand, as well as obtain measurements in a variety of finger positions and locations. The minimum baseline forces are stored and used as a compensatory feedforward term in the glove controller. After the calibration, the glove will automatically change the state to Main Idle while keeping the fingers at the neutral position. The Calibration progression of passive hand and finger exercises can be repeated as necessary at the user’s pace in order to enact a full passive rehabilitation session.

Once in the Active Rehabilitation/Assistance state machine, the program proceeds through a sequence of substates, as seen as Fig. 5. The initial substate is the Control Idle substate. In this substate, the fingers will remain at rest at the current position, and the glove will wait for a twitch signal. Once an

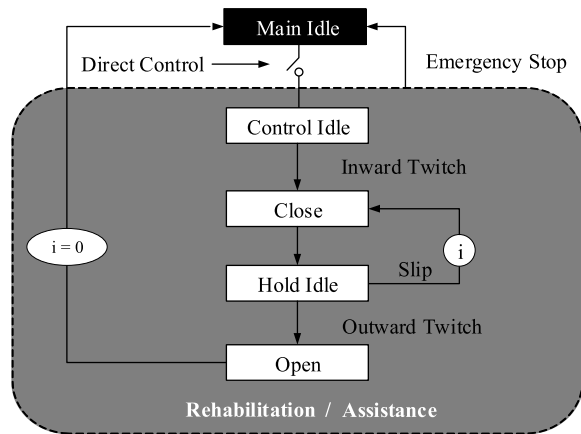


Fig. 5. Rehabilitation/Assistance state machine detail.

inward twitch signal is detected, a substate change is triggered and the glove proceeds to the Close substate.

The Close substate contains closed-loop hysteresis force controllers utilized to flex each finger independently until the force reference is reached for all. A hysteresis controller was utilized due to its optimality for applications that require the fastest possible response [30]. The use of multiple controllers enables geometrically adaptive grips to interact with objects of varying shape. Upon the first such iteration through the Close substate, the initial force input is utilized to control the first grip, and this ‘initial soft grip force’ is experimentally determined through interaction with compliant objects. The controller then outputs a PWM signal to the motor for each finger until the initial soft grip force input is reached. Once the force input has been realized, the program proceeds to the Hold Idle substate, wherein the position is held and slip detection routine is activated. If slip is detected, the glove then returns to the Close substate, increasing the force input and velocity reference in a stepwise manner in order to grip more firmly and quickly in the event of successive slip events. The program again then returns to the Hold Idle substate. This sequence continues until slip is no longer detected, with the force reference increasing with each iteration. A diagram depicting a single finger’s controller is shown in Fig. 6. The controller and force reference equations are as follows:

$$F_{IN} = F_{FF} + F \cdot i \quad (1)$$

$$v_{ref} = \begin{cases} v_{FF} + v \cdot i, & \text{if } e > 0 \\ 0, & \text{if } e \leq 0 \end{cases} \quad (2)$$

where F_{IN} is the stepwise input force, F_{FF} is the ‘initial soft grip force’, F is the force increase gain, v_{ref} is the velocity reference, v_{FF} is the initial velocity, v is the velocity increase gain, e is the error as measured by $F_{IN} - F_{feedback}$ and i is the iteration feedback that drives the increase in the stepwise force and velocity functions.

If an outward twitch is detected, the system then proceeds to the Open substate. Here, the fingers extend to an open hand position using a closed-loop hysteresis position controller, utilizing feedback from potentiometers located on the finger joints. The force references and substate iteration counters

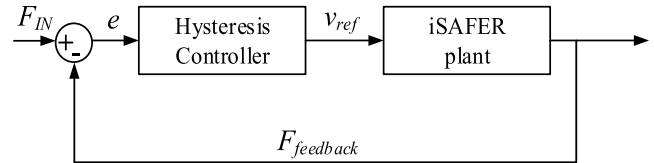


Fig. 6. Force control diagram in close substate.

are reinitialized to zero. Once the open position is achieved, program returns to Main Idle.

IV. SENSORY DATA ANALYSIS

The sensory stream provided by the array of sensors embedded within the glove’s design provides a rich feedback environment. This data is utilized for multiple purposes, including setting fail-safe protections for the wearer, sensing motion commands, and detecting and analyzing contact forces when the glove is used to grasp an object.

A. Tracking of the Finger Position

Where each finger linkage joins the dorsal plate, a rotary potentiometer tracks the angular position. Using this data allows for the tracking of the finger through the kinematic relations of the cabling system. The main application of tracking the finger position is to ensure the safety of the wearer and protect their fingers from being extended beyond the set limits. During the Calibration state, the fingers are gently guided from full flexion to full extension, at which time the limits on the motion of the joints can be adjusted as necessary to ensure an ideal fit as well as to maintain wearer comfort.

B. Measurement of Finger Forces

In order to verify the operation of the new FSCE sensors, data was recorded while grasping a paper cup, and analyzed in order to confirm that the performance matched or exceeded that of the previously reported system [25].

In Fig. 7 above, 30 grasps were performed with the glove recording force data passively. The data presented are the results from just one finger, depicted in a raw form in the top image in Fig. 7. Utilizing dynamic time warping (DTW) in order to temporally align the various grasp sequences, as in [25], the feedback shows strong resemblance to the previously reported data, with greater force resolution and detail. While the performance between sensors is comparable, the new FSCE is superior in terms of flexibility and thus conformance to the finger for a more accurate force profile for the fingertip, resilience against breakage, and cost. Thus, the new FSCE sensors demonstrate a robust improvement on the previous system.

The grip demonstration data shown above was collected while a healthy user was gently grasping and lifting an empty paper cup. As such, an average of peak grasp force from the trials is implemented as the initial soft grip force in the system, providing a low initial contact force for the glove in order to enable interaction with compliant objects.

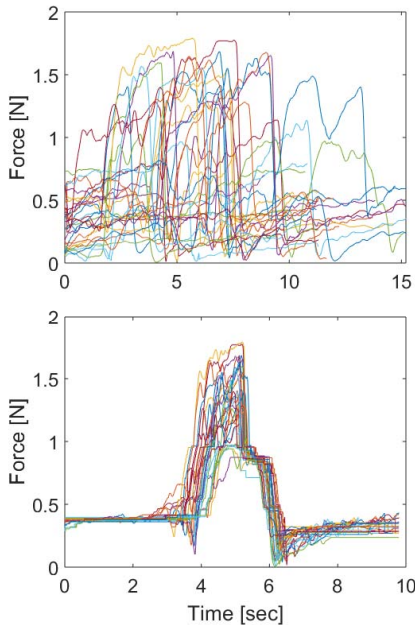


Fig. 7. Index force data from new sensor (top) raw data (bottom) DTW result.

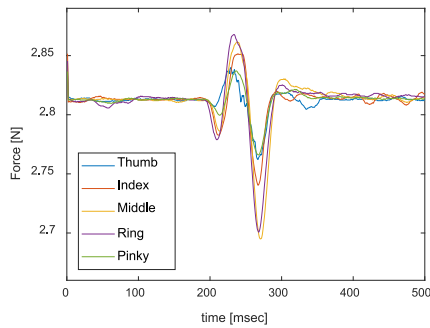


Fig. 8. Inward twitch force feedback characteristics of fingers.

C. Motion Amplification

The main activation method of motion amplification requires the detection of finger motion by the wearer. In order to test the sensitivity of the method as well as to demonstrate the applicability for patients with minimal hand functionality, the activation limit is designed to trigger at a minor twitch in the most sensitive configuration. The force feedback resulting from a user flexional twitch followed by a return to starting hand position while wearing the glove is depicted in Fig. 8, with the data from each finger normalized about a common mean initial value for readability. While the signal is oscillatory, the major feature is the positive force impulse, indicating an increase in force in the direction of finger flexion. The following negative impulse is driven by the elastic properties of the FSCE materials.

In order to detect the positive impulse associated with a flexional twitch, positive derivative detection logic is utilized to trigger a state change. While the glove is in the Control Idle substate, the data from the FSCE sensors for each finger are central differentiated in real time. Utilizing the user twitch data such as that depicted in Fig. 8, a positive derivative limit of

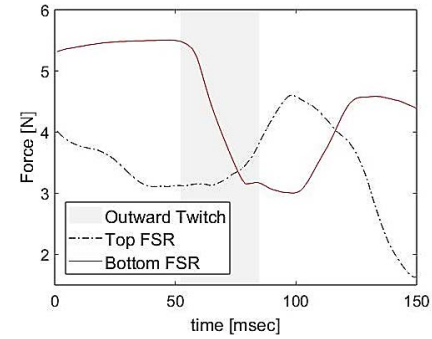


Fig. 9. Outward twitch force feedback characteristics of fingers.

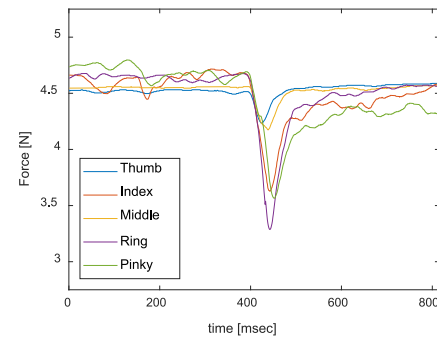


Fig. 10. Slip event force feedback characteristics of fingers.

.012 N over 10 ms was determined. If the differentiated value is found to exceed the twitch slope limit, the progression to the “Close” substate is triggered.

In Fig. 9, the force characteristics utilized for the outward twitch motion detection are shown. Unlike inward twitch or slip detection, the outward force change is measured through monitoring both the top and bottom FSCE sensors for each finger. In this case, the bottom force reading decreases as it loses contact with the finger, while the top sensor detects a slight increase. Similar to the inward twitch, derivative limits are set. The outward twitch is detected while the program is in the Hold Idle substate, and the top FSCE sensor crosses the positive derivative threshold while the bottom simultaneously crosses the negative. In the Fig. 9, the twitch can be seen to occur within the grey shaded area.

D. Slip Detection

Insufficiently stable grip configurations must be detected to dynamically adjust the grip assistance supplied by the glove. Research on the tangential forces during slip situations for human grips has shown that the advent of a slip event is indicated by a sudden drop in normal force [31]. Experimental data collected from the fingertip FSCE sensors of the iSAFER glove in generated slip events corroborate these findings, as shown in Fig. 10.

This event signature can thus be incorporated into the state machine in order to trigger a state change when a poor grip configuration is detected. While in the Hold Idle substate, the central difference of the data from the FSCE sensors is compared to a negative derivative force limit, computed

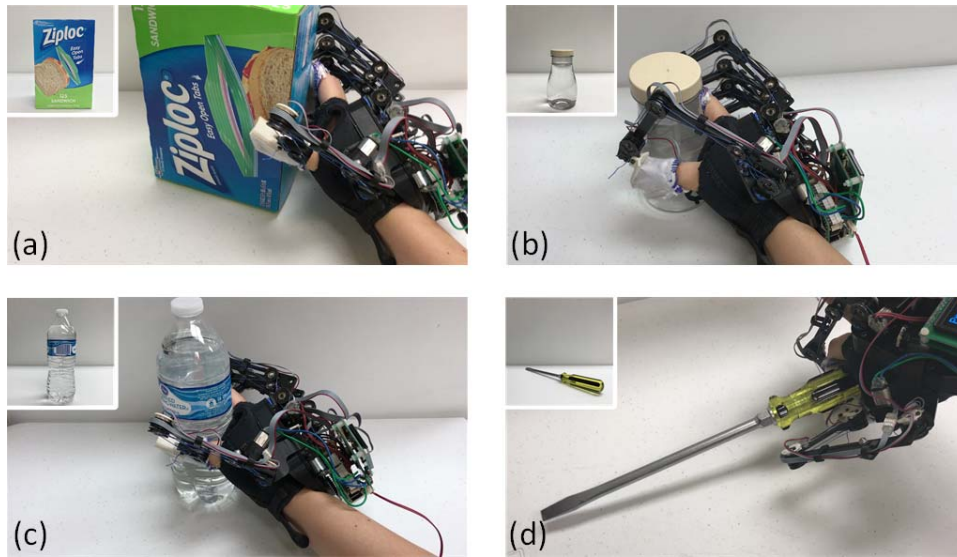


Fig. 11. Four objects of different shapes and textures for the experiments: (a) cardboard box, (b) variable diameter cylinder, (c) water bottle, (d) screw driver.

from aggregated experimentally-generated slip events. If the approximated force derivative from a finger is found to drop below the derivative limit, a state change is thus triggered and the glove proceeds to the Close substate. Once complete, the glove returns to the Hold Idle state, where it again can detect any slip events. This state cycle will repeat until a secure grasp is realized, with the reference force incrementing upward monotonically.

V. EXPERIMENTS

After defining the characteristics of the twitch, slip, and initial soft grip force values, the system was first validated through the feedback from a single finger, and a cylindrically shaped object with a smooth surface. Once validated, that experiment was expanded to four more objects of different shapes and textures, shown in Fig. 11. The weight of each of the four objects was as follows: (a) 322 g, (b) 350 g, (c) 513 g, and (d) 238 g.

The data was collected from all five FSCE sensors and the analysis is presented below. Previous work with this platform often used a wooden hand to represent the impaired hand for experimentation. However, in order to perform the twitch activation and accurately illustrate the degrees of freedom possessed by a human hand, the wooden mannequin hand was insufficient. Thus, in the following, a human participant with healthy hands was told to initiate the closing motion by producing short twitch motion, but not to apply any force while grabbing the object.

Utilizing the grasp taxonomy system developed by Feix in [32], for Objects (a)-(d), the iSAFER glove performed a parallel extension grasp, a large diameter grasp that transitions to a small diameter grasp as the object slips to its tapered top, a medium wrap grasp, and a ring grasp, respectively. The glove acts by actuating all five fingers to securely lift the objects off the table. The individually force controlled fingers

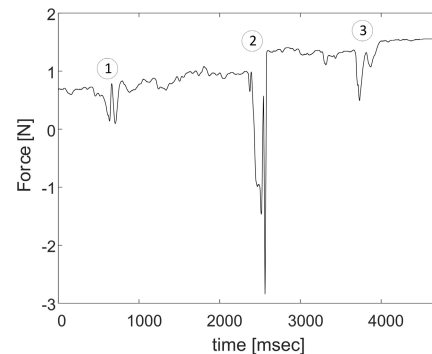


Fig. 12. Force feedback profile for a single finger grasping a cylindrical object.

allow the system to overcome variations in object geometry and adaptively conform to the object as necessary.

A. Intelligent Object Grasping

The single finger validation experiment proved the glove was able to perform both the soft grip and detect slippage. Once the slip detection triggers the Close substate, incrementally increasing force was applied to the object to compensate the weight of the object in order to grip it securely. The result of the experiment is illustrated in Fig. 12. This figure depicts the entire sequence of a grasp, from twitch input to secure grasp. Event 1 marks where the twitch input is received and the force applied by the glove can be seen to increase. Event 2 then shows the first slip occurrence following the achievement of the soft grasp force. This slip had a much larger drop in normal force than the second slip, indicated by Event 3. As more force was applied to stabilize the grasp, the drop force reduced as well as the noise in the force.

The cylindrical shape of the grasped object lends itself to the shown force profile, as the uniform diameter results in a roughly stepwise force increase as the grasp is secured. This is

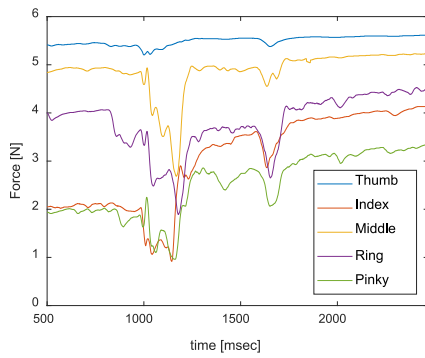


Fig. 13. Force feedback profile for five fingers grasping a cylindrical object.

a clear illustration of the stepwise reference force function and the hysteresis controller's quick response to the slip events, as designed.

B. Five Finger Object Interaction

While wearing the glove, the user first performed the calibration exercises in order to correctly calculate the initial force offsets due to finger geometry. Once calibrated, the program proceeded to the active rehabilitation and assistance state machine, wherein the human participant attempted to grasp the desired object. When the twitch motion was produced by the wearer, the glove detected the twitch and initiated flexion. Following the initial flexion, the glove stopped closing when the soft grip force was detected. Soon after, when the human participant tried to lift the object, the occurrence of slip triggered closing until it met new limit. In Fig. 13 below, the grasp interaction between the wearer and the cylindrical validation object is depicted for all five fingers.

The five-finger twitch can be seen at 1100 msec, at which time the finger flexion is triggered. At 1600 msec, a slip event can be seen to occur, at which time the controller recognizes this and proceeds to close the fingers and increase the grip force. A small spike in normal force can be observed prior to the slip-induced force drop. This is due to the object's overcoming of static friction prior to slippage.

It can be seen that the four fingers have very similar force profiles. As the grasped object is cylindrical and thus necessitated a medium wrap grasp, the majority of the oppositional force is palmar. The thumb does provide the largest force, due to its oppositional nature in a cylindrical grasp. However, as the proximal phalange of the thumb as well as the webbing of the hand are also in contact with the object, the tip force measurements of the thumb do not show an oppositional force equal to the sum of the other fingers. A future improvement for the sake of grip force analysis is the addition of a palmar force-sensing array to provide a more comprehensive force characterization.

C. Multi-Object Grasp Experiment

In Fig. 14 below, data is presented comparing the force profiles of the grasps of the four experimental objects shown in Fig. 11. Force data from a single finger in each case is

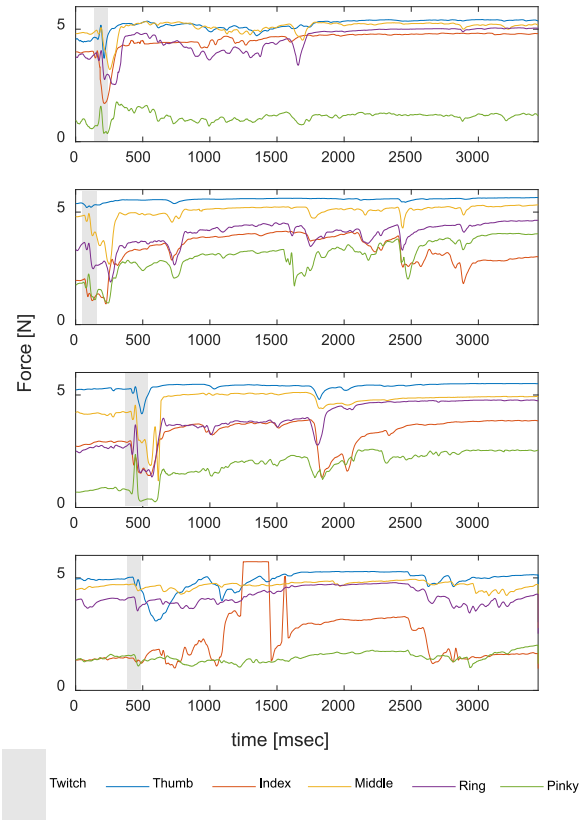


Fig. 14. Force feedback profile for four objects: (a) cardboard box, (b) variable diameter cylinder, (c) water bottle, and (d) screwdriver.

presented for readability. The twitch commands are indicated by the grey shaded area at the initial motion. Following the twitch command, a momentary drop in force can be observed. This is caused by the beginning of the iSAFER glove's finger flexion motion, in concert with the elastic effects of the FSCE. As the linkages push the backside of the fingers toward a closed grip, the contact exerted by the finger upon the pad FSCE decreases below the calibrated offset, until the fingers make contact with the object and the force again increases.

The increasing reference force can be clearly seen following each slip event. The quick response of the slip recovery can also be seen in the short time difference between the start of a slip and the corresponding force increase. In addition, the wearer finished each trial by lifting the object from the table, and the force feedback at the final state is thus directly proportional to the mass of the objects. This is clearly shown by the final recorded values for each object.

The effect of the geometrical shape of the grasped objects on the grasp force is also illustrated by the data. For instance, Object (b), the variable diameter cylinder, shows two significant slip events at 1600 and 2500 msec as well as two anomalous smaller slip events at 2200 and 3000 msec. The smaller events occur when the objects shift within the glove to a smaller diameter section, resulting in a slower decrease in normal force, followed by a sudden initiation of slip that triggers the closing controller of the glove. The variable diameter also causes the much higher degree of noise in the normal force feedback. Similarly, Object (a), the cardboard

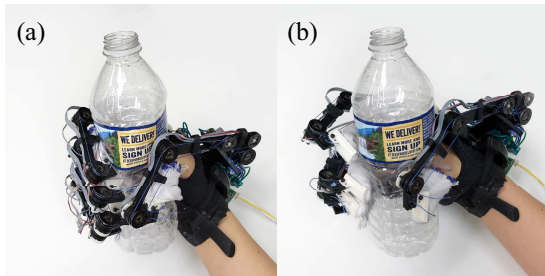


Fig. 15. (a) SAFER system, (b) iSAFER system with intelligent object grasping.

box, shows a high level of normal force noise early on in the grip, prior to the firmer grip following the slip event. This is driven by the slight deformation of the box as it is gripped until a firm grip is achieved.

In addition, it can be seen that for the constant width or diameter Objects (a) and (c), the box and the water bottle, the iSAFER glove only required one major slip event and subsequent finger closure to achieve a stable grip upon the object. However, for the non-uniform diameter of Object (b), the variable diameter cylinder, multiple slip events are required in order to stabilize the grip. These slip events can be seen to have varying magnitude, as with each event the diameter of the object being gripped changes, resulting in decreased contact between the iSAFER glove and the object, which the system then compensates for. Furthermore, the data presented shows that with the uniform Objects (a) and (c), the iSAFER glove reaches a steady-state secure grip more quickly than while interacting with a non-uniform object. This holds with the expected results, as greater object complexity would at times require more grip closures in order to achieve a stable grasp.

In performing a ring grasp to pick up Object (d), the screwdriver, the iSAFER glove demonstrated that its slip adaptive grasping can also be applied to grips beyond full hand grasps. The major slip event at 1100 msec is followed by a recovery and the noisy force feedback period where the screwdriver shifts within the grip of the glove. The force measurements of middle, ring and pinky fingers can be seen to remain mostly stable as the only forces sensed are due to the motion of the fingers with the finger thimbles. The index finger sensor can be seen to saturate and then fall off at the screwdriver rotated within the grip until it only made tangential contact on the sensor and was supported by the lower, sensorless section of the finger. This can be remedied through the inclusion of larger FSCEs to cover more of the finger.

D. Deformable Object Grasp Experiment

In addition to the four objects used in previous experiments, an empty water bottle was used to test the intelligent object grasping with a deformable object. Fig. 15 shows the difference in result between the SAFER system and the iSAFER system introduced in this paper. Previously, SAFER was programmed to have simple force control with a static reference force. Therefore, its grasp crushed the deformable

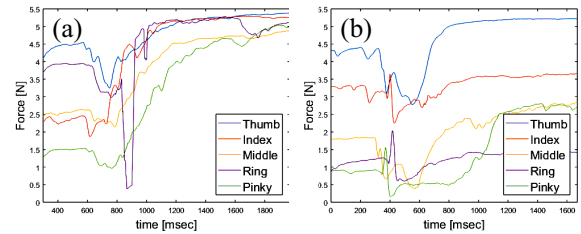


Fig. 16. Force feedback for five fingers of: (a) SAFER, and (b) iSAFER system.

object as shown in Fig. 15(a) while flexing all fingers to reach the reference force as required by the original SAFER controller, as shown in Fig. 16(a) [25]. When the iSAFER system with intelligent object grasping was used to pick up the empty water bottle, the iSAFER system stopped closing once the FSCE sensors touched the surface and reached the soft contact force as shown in Fig. 15(b) and Fig. 16(b). As the bottle itself only weighed 10g, the slip event did not occur, and the initial soft grasping force was firm enough to hold the bottle.

VI. CONCLUSION AND FUTURE WORK

This paper presented an intelligent controller that utilized slip-aware grasping in order to provide an adaptive force profile for the robotic glove exoskeleton fingers. By sensing variations in the normal force between the fingers and the object grasped, the glove was able to detect slip and adaptively recover in situations in which the object began to fall from the hand.

The glove can provide both passive rehabilitation exercise as well as active grasping rehabilitation and assistance. This widens the applicability of the system as a rehabilitative and assistive device. The use of a soft grip force enables the system to interact with delicate objects, while also adapting the grasp force as needed for heavier objects.

In future work, improved sensing and automation capabilities will be explored. Though the analysis of force data at the finger pads was enough to activate the iSAFER system, the addition of a sensory array on the palm of the wearer's hand will provide improved force profiles and drive further grasp adaptability. In this study, the pressure distribution map of the hand and the deformation of the skin at contact can be considered [33]. Integration of artificial neural networks can utilize wearer data to provide decreased response time in order to achieve a stable grip upon identification of the geometric profile of the object via the feedback provided by the potentiometer, while also learning and adapting to the capabilities of the wearer as their abilities improve throughout rehabilitation. Clinical trials with a variety of participants will be conducted in order to provide a more detailed analysis of the system's rehabilitation capabilities in the future.

REFERENCES

- [1] G. B. Prange, M. J. A. Jannink, C. G. M. Groothuis-Oudshoorn, H. J. Hermens, and M. J. IJzerman, "Systematic review of the effect of robot-aided therapy on recovery of the hemiparetic arm after stroke," *J. Rehabil. Res. Develop.*, vol. 43, no. 2, pp. 171–184, 2006.

- [2] R. Riener *et al.*, "A view on VR-enhanced rehabilitation robotics," in *Proc. Int. Workshop Virtual Rehabil.*, Aug. 2006, pp. 149–154.
- [3] J. Lee and P. Ben-Tzvi, "Design of a wearable 3-DOF forearm exoskeleton for rehabilitation and assistive purposes," in *Proc. ASME Int. Mech. Eng. Congr. Expo. (IMECE)*, vol. 3, 2017, p. V003T04A078.
- [4] E. Refour, B. Sebastain, and P. Ben-Tzvi, "Design and integration of a two-digit exoskeleton glove," in *Proc. ASME Int. Design Eng. Tech. Conf. Inf. Comput. Eng. Conf. (IDETC/CIE)*, 2017, p. V05AT08A058.
- [5] B. R. Brewer, S. K. McDowell, and L. C. Worthen-Chaudhari, "Post-stroke upper extremity rehabilitation: A review of robotic systems and clinical results," *Topics Stroke Rehabil.*, vol. 14, no. 6, pp. 22–44, 2007.
- [6] M. Gobbo *et al.*, "Hand passive mobilization performed with robotic assistance: Acute effects on upper limb perfusion and spasticity in stroke survivors," *Biomed Res. Int.*, vol. 2017, Sep. 2017, Art. no. 2796815.
- [7] M. A. Diftler *et al.*, "RoboGlove—A grasp assist device for earth and space," in *Proc. 45th Int. Conf. Environ. Syst.*, Jul. 2015, pp. 1–8.
- [8] P. Polygerinos, Z. Wang, K. C. Galloway, R. J. Wood, and C. J. Walsh, "Soft robotic glove for combined assistance and at-home rehabilitation," *Robot. Auto. Syst.*, vol. 73, pp. 135–143, Nov. 2015.
- [9] P. Ben-Tzvi and Z. Ma, "Sensing and force-feedback exoskeleton (SAFE) robotic glove," *IEEE Trans. Neural Syst. Rehabil. Eng.*, vol. 23, no. 6, pp. 992–1002, Nov. 2015.
- [10] E. D. Engeberg and S. G. Meek, "Adaptive sliding mode control for prosthetic hands to simultaneously prevent slip and minimize deformation of grasped objects," *IEEE/ASME Trans. Mechatronics*, vol. 18, no. 1, pp. 376–385, Feb. 2013.
- [11] I. Jo and J. Bae, "Design and control of a wearable and force-controllable hand exoskeleton system," *Mechatronics*, vol. 41, pp. 90–101, Feb. 2017.
- [12] Z. Su *et al.*, "Force estimation and slip detection/classification for grip control using a biomimetic tactile sensor," in *Proc. IEEE-RAS Int. Conf. Humanoid Robot.*, Nov. 2015, pp. 297–303.
- [13] R. M. Crowder, V. N. Dubey, P. H. Chappell, and D. R. Whatley, "A multi-fingered end effector for unstructured environments," in *Proc. IEEE ICRA*, vol. 4, May 1999, pp. 3038–3043.
- [14] A. A. S. Al-Shanoon, S. A. Ahmad, and M. K. B. Hassan, "Slip detection with accelerometer and tactile sensors in a robotic hand model," *IOP Conf. Ser., Mater. Sci. Eng.*, vol. 99, no. 1, p. 12001, Nov. 2015.
- [15] L. Roberts, G. Singhal, and R. Kaliki, "Slip detection and grip adjustment using optical tracking in prosthetic hands," in *Proc. Annu. Int. Conf. IEEE Eng. Med. Biol. Soc. (EMBS)*, Aug./Sep. 2011, pp. 2929–2932.
- [16] R. Fernandez, I. Payo, A. S. Vazquez, and J. Becedas, "Slip detection in robotic hands with flexible parts," in *Proc. 1st Iberian Robot. Conf. Adv. Intell. Syst. Comput. (ROBOT)*, vol. 253, 2014, pp. 153–167.
- [17] Z. Ma and P. Ben-Tzvi, "Tendon transmission efficiency of a two-finger haptic glove," in *Proc. IEEE Int. Symp. Robotic Sensors Environ. (ROSE)*, Oct. 2013, pp. 13–18.
- [18] Z. Ma and P. Ben-Tzvi, "RML glove—An exoskeleton glove mechanism with haptics feedback," *IEEE/ASME Trans. Mechatronics*, vol. 20, no. 2, pp. 641–652, Apr. 2015.
- [19] Z. Ma and P. Ben-Tzvi, "Design and optimization of a five-finger haptic glove mechanism," *J. Mech. Robot.*, vol. 7, no. 4, p. 41008, 2015.
- [20] Z. Ma, P. Ben-Tzvi, and J. Danoff, "Modeling human hand and sensing hand motions with the five-fingered haptic glove mechanism," in *Proc. ASME Int. Design Eng. Tech. Conf. Comput. Inf. Eng. Conf. (IDETC/CIE)*, 2014, p. V05AT08A008.
- [21] P. Ben-Tzvi, J. Danoff, and Z. Ma, "The design evolution of a sensing and force-feedback exoskeleton robotic glove for hand rehabilitation application," *J. Mech. Robot.*, vol. 8, no. 5, p. 51019, 2016.
- [22] Z. Ma and P. Ben-Tzvi, "An admittance glove mechanism for controlling a mobile robot," in *Proc. ASME Int. Design Eng. Tech. Conf. Comput. Inf. Eng. Conf. (IDETC/CIE)*, 2012, pp. 1109–1114.
- [23] Z. Ma, P. Ben-Tzvi, and J. Danoff, "Sensing and force-feedback exoskeleton robotic (SAFER) glove mechanism for hand rehabilitation," in *Proc. ASME Int. Design Eng. Tech. Conf. Comput. Inf. Eng. Conf. (IDETC/CIE)*, vol. 8, no. 5, 2015, p. V05AT08A036.
- [24] Z. Ma and P. Ben-Tzvi, "An admittance type haptic device: RML glove," in *Proc. ASME Int. Mech. Eng. Congr. Expo. (IMECE)*, 2011, pp. 1219–1225.
- [25] Z. Ma, P. Ben-Tzvi, and J. Danoff, "Hand rehabilitation learning system with an exoskeleton robotic glove," *IEEE Trans. Neural Syst. Rehabil. Eng.*, vol. 24, no. 12, pp. 1323–1332, Dec. 2016.
- [26] U. Naqvi and A. L. Sherman, "Muscle strength grading," vol. 12, no. 6, 2017.
- [27] S. Hesse, G. Schulte-Tiggens, M. Konrad, A. Bardeleben, and C. Werner, "Robot-assisted arm trainer for the passive and active practice of bilateral forearm and wrist movements in hemiparetic subjects," *Arch. Phys. Med. Rehabil.*, vol. 84, no. 6, pp. 915–920, Jun. 2003.
- [28] M. L. Aisen *et al.*, "The effect of robot-assisted therapy and rehabilitative training on motor recovery following stroke," *Arch. Neurol.*, vol. 54, no. 4, pp. 443–446, Apr. 1997.
- [29] R. S. Johansson and J. R. Flanagan, "Coding and use of tactile signals from the fingertips in object manipulation tasks," *Nature Rev. Neurosci.*, vol. 10, no. 5, pp. 345–359, 2009.
- [30] Z. Shen and S. B. Andersson, "Minimum time control of a second-order system," in *Proc. 49th IEEE Conf. Decis. Control*, vol. 2, no. 1, Dec. 2010, pp. 4819–4824.
- [31] H. Kinoshita, L. Bäckström, J. R. Flanagan, and R. S. Johansson, "Tangential torque effects on the control of grip forces when holding objects with a precision grip," *J. Neurophysiol.*, vol. 78, no. 3, pp. 1619–1630, 1997.
- [32] T. Feix, J. Romero, H.-B. Schmiedmayer, A. M. Dollar, and D. Kragic, "The GRASP taxonomy of human grasp types," *IEEE Trans. Human-Mach. Syst.*, vol. 46, no. 1, pp. 66–77, Feb. 2016.
- [33] Y. Xie, S. Kanai, and H. Date, "An efficient simulation of skin Conta CT deformation for virtual ergonomic assessments of handheld products," *Int. J. CAD/CAM*, vol. 13, no. 1, pp. 81–95, 2013.